Origin of the Difference in Proton Transport Direction between Inward and Outward Proton-Pumping Rhodopsins

*Taito Urui and Yasuhisa Mizutani**

Department of Chemistry, Graduate School of Science, Osaka University, 1-1 Machikaneyama, Toyonaka, Osaka 560-0043, Japan

KEYWORDS

Microbial rhodopsin, proton transfer, resonance Raman spectroscopy, time-resolved spectroscopy

Conspectus

Active transport is a vital and ubiquitous process in biological phenomena. Ion-pumping rhodopsins are light-driven active ion transporters, which share a heptahelical-transmembrane structural scaffold in which the all-*trans* retinal chromophore is covalently bonded through a Schiff base to a conserved lysine residue in the seventh transmembrane helix. Bacteriorhodopsin from *Halobacterium salinarum* was the first ion-pumping rhodopsin to be discovered and was identified as an outward proton-pumping rhodopsin. Since the discovery of bacteriorhodopsin in 1971, many more ion-pumping rhodopsins have been isolated from diverse microorganisms spanning three domains (bacteria, archaea, and eukaryotes) and giant viruses. In addition to proton-pumping rhodopsins, chloride ion- and sodium ion-pumping rhodopsins have also been discovered. Furthermore, diversity of ion-pumping rhodopsins was found in the direction of ion transport, i.e., rhodopsins that pump protons *inwardly* have recently been discovered. Very intriguingly, the inward proton-pumping rhodopsins share structural features and many conserved key residues with the outward proton-pumping rhodopsins. Yet, a central question remains unchanged despite the increasing variety: how and why do the ion-pumping rhodopsins undergo interlocking conformational changes that allow unidirectional ion transfer within proteins? In this regard, it is an effective strategy to compare the structures and their evolutions in the proton-pumping processes of both inward and outward proton-pumping rhodopsins because the comparison sheds light on key elements for the unidirectional proton transport. We elucidated the proton-pumping mechanism of the inward and outward proton-pumping rhodopsins by time-resolved resonance Raman spectroscopy, a powerful technique for tracking the structural evolutions of proteins at work that are otherwise inaccessible.

In this Account, we primarily review our endeavors in the elucidation of the proton-pumping mechanisms and determination factors for the transport directions of inward and outward proton-pumping rhodopsins. We begin with a brief summary of previous findings on outward proton-pumping rhodopsins revealed by vibrational spectroscopy. Next, we provide insights into the mechanism of inward proton-pumping rhodopsins, schizorhodopsins, obtained in our studies. Time-resolved resonance Raman spectroscopy provided valuable information on the structures of the retinal chromophore in the unphotolyzed state and intermediates of schizorhodopsins. As we ventured further into our investigations, we succeeded in uncovering the factors determining the directions of proton release and uptake in the retinal Schiff base. While it is intriguing that the proton-pumping rhodopsins actively transport protons against a concentration gradient, it is even more curious that proteins with structural similarities transport protons in opposite directions. Solving the second mystery led to solving the first. When we considered our findings, we realized that we would probably not have been able to elucidate the mechanism if we had studied only the outward pump. Our Account concludes by outlining future opportunities and challenges in the growing research field of ion-pumping rhodopsins, with a particular emphasis on elucidating their sequence-structure-function relationships. We aim to inspire further advances toward the understanding and creation of light-driven active ion transporters.

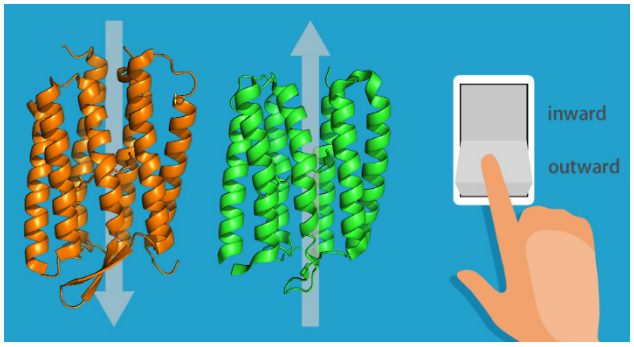

Key References

- Shionoya, T.; Singh, M.; Mizuno, M.; Kandori, H.; Mizutani, Y., Strongly Hydrogen-Bonded Schiff Base and Adjoining Polyene Twisting in the Retinal Chromophore of Schizorhodopsins. *Biochemistry* **2021,** *60*, 3050-3057.[1]
  This paper is the first report on resonance Raman spectra of schizorhodopsins, providing in-depth insights into the chromophore structure in their unphotolyzed state.
- Hayashi, K.; Mizuno, M.; Kandori, H.; Mizutani, Y., *Cis–Trans* Reisomerization Precedes Reprotonation of the Retinal Chromophore in the Photocycle of Schizorhodopsin 4. *Angew. Chem. Int. Ed.* **2022,** *61*, e202203149.[2]
  This paper presents experimental evidence of an unprecedented sequence of the structural evolution in the retinal chromophore, which well explains proton uptake from the extracellular medium in the inward proton transport.
- Urui, T.; Hayashi, K.; Mizuno, M.; Inoue, K.; Kandori, H.; Mizutani, Y., *Cis–Trans* Reisomerization Preceding Reprotonation of the Retinal Chromophore Is Common to the Schizorhodopsin Family: A Simple and Rational Mechanism for Inward Proton Pumping. *J. Phys. Chem. B* **2024,** *128*, 744-754.[3]
  This paper provides in-depth insights into the reisomerization preceding reprotonation of the retinal chromophore, demonstrating that a simple and rational mechanism for inward proton transport of schizorhodopsins.
- Urui, T.; Shionoya, T.; Mizuno, M.; Inoue, K.; Kandori, H.; Mizutani, Y., Chromophore–Protein Interactions Affecting the Polyene Twist and π–π* Energy Gap of the Retinal Chromophore in Schizorhodopsins. *J. Phys. Chem. B* **2024,** *128*, 2389-2397.[4]
  This paper reports correlations of structural features and reisomerization rate of schizorhodopsins, shedding light on functional significance of the tight atomic contacts and the hydrogen bond of the Schiff base on the chromophore.

1. Introduction

Active ion transport across biological membranes is essential for energy conversion, homeostasis, and environmental sensing.[5] This process involves the relay of ions within proteins, which requires interlocked conformational changes that can be viewed as molecular machinery. The unidirectionality of the ion relay against a concentration gradient is a fundamental principle governing active transport by membrane transporter proteins. How the ion relay direction is controlled in the protein is a key question for understanding the mechanism of active ion transport.

Ion-pumping rhodopsins are a fascinating group of proteins that demonstrate a close relationship between structural changes and functionality. These proteins utilize light energy to facilitate ion transport across cellular membranes.[6-7] The study of ion-pumping rhodopsins began with the identification of bacteriorhodopsin, a proton pump, in the halophilic archaeon *Halobacterium salinarum* (*Hs*BR).[8-9] Following this discovery, researchers identified various other pumps for protons, chloride ions,[10-11] and sodium ions[12-13] in organisms spanning all three domains of life, as well as in viral genes.[14-15] Interestingly, despite sharing similar structural characteristics, these ion-pumping rhodopsins exhibit diverse ion-transporting capabilities. Their structure consists of a polypeptide chain that forms a seven-transmembrane domain structure known as opsin (Figure 1), along with retinal, which is covalently attached to a conserved lysine residue in the opsin via a protonated Schiff base linkage.

The variety of ion-pumping rhodopsins has expanded to another dimension: the direction of proton transport. From the discovery of *Hs*BR in 1971 to 2016, all the proton-pumping rhodopsins discovered were outward proton pumps. Therefore, the 2016 discovery of an inward proton pump (*Po*XeR) from the deep-ocean marine bacterium *Parvularcula oceani* was a great

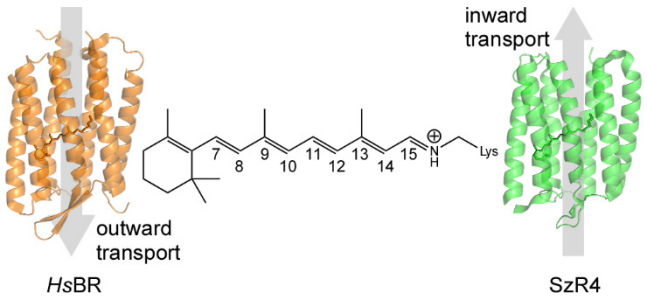

Figure 1. Protein structures of *Hs*BR (PDB ID: 1C3W) and SzR4 (PDB ID: 7E4G) and their retinal chromophores with position numbering of the skeletal carbon atoms.

surprise.[16] Schizorhodopsin (SzR) is a newly identified subfamily of rhodopsins found in the genome sequences of Asgard archaea, which are believed to be the closest extant prokaryotes to the last common ancestor of eukaryotes.[17] The first SzRs discovered were shown to function as light-driven inward proton pumps. Later, more SzRs were found from archaeal species living in high-temperature environments and were also identified as inward proton-pumping rhodopsins.[18] A newly discovered inward proton-pumping rhodopsin identified in metagenomic sequences obtained from Antarctic freshwater lakes shares a close phylogenetic relationship with SzR.[19] It is highly intriguing that the SzRs transport protons inwardly despite having structural features and membrane topology that are characteristic of outward proton pumps.[20]

In Section 3 of this Account, we describe the chromophore structures of the unphotolyzed state and intermediates of SzR AM_5_00977 (SzR4), comparing them with the structures of *Hs*BR that are discussed in Section 2. Comparison of the proton-pumping mechanisms of the two pumps and mechanisms of unidirectional proton transfer are discussed in Sections 4 and 5, respectively. In Section 6, roles of the protonated Schiff base in the ion transport are discussed for inward and outward proton-pumping, chloride ion-pumping, and sodium ion-pumping rhodopsins. Finally, in Section 7, we discuss future perspectives for studies on ion-pumping rhodopsins.

2. Proton Transport Mechanism of Bacteriorhodopsin: Outward Proton Pump

Far more insights have been accumulated on outward proton pumps compared to inward proton pumps. Due to their similarities, an overview of outward proton-transporting mechanisms is the logical starting point to understand the transport mechanism of inward proton pumps. In this regard, we will discuss the proton-transporting mechanism of *Hs*BR, which is the best studied outward proton pump.

Ion-pumping rhodopsins undergo a cyclic reaction, called a photocycle, which is triggered by photoisomerization of the retinal chromophore from the all-*trans* to the 13-*cis* configuration, and involves a series of spectrally distinct intermediates (Figure 2A). During the photocycle, the retinal chromophore undergoes changes that drive corresponding conformational changes in opsin, facilitating ion translocation.

The key aspect of the photocycle is the chromophore structure of the intermediates, since the photocycle is initiated by the photoexcitation of the chromophore and the Schiff base of the chromophore serves as a relay point for proton transfer in the protein. Resonance Raman (RR) spectroscopy substantially contributed to the elucidation of chromophore structures in the photocycle of *Hs*BR. RR spectra of the isotopically labeled chromophore in *Hs*BR were collected and normal mode analysis was carried out for the unphotolyzed state of *Hs*BR for

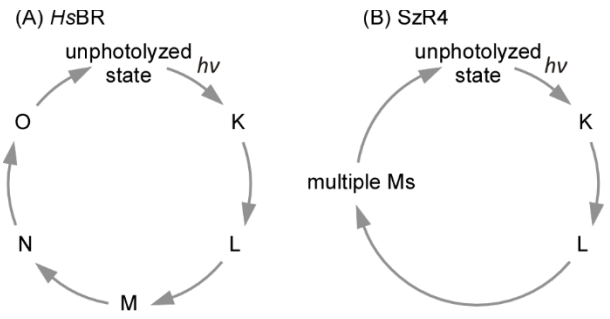

Figure 2. Photocycles of *Hs*BR (A) and SzR4 (B).

vibrational assignments of Raman bands from the chromophore.[21-22] It was shown that the unphotolyzed form of light-adapted *Hs*BR has a retinal chromophore with a protonated Schiff base in the all-*trans* configuration.[23] Configurations of the K, L, M, and N intermediates were shown to have the chromophore in the 13-*cis* form. In the O intermediate, the chromophore adopts the all-*trans* form, the same as in the unphotolyzed form. The Schiff base is deprotonated only in the M intermediate while it is protonated in all the other intermediates.

Amino acid residues of the relay points for the proton transport were identified by IR spectroscopy. The residues involved in proton transfer are hypothesized to be those with carboxyl groups. Strong IR absorptions caused by carbonyl stretching vibrations of the carboxylic and carboxylate groups are observed at 1700–1780 and 1300–1420 cm^{-1} (symmetric stretching), respectively. Therefore, it is convenient to examine the protonation states of the side chains of these residues. Pioneering work was conducted by Rothschild et al.[24] and Siebert et al.,[25] where spectral changes in the IR absorption spectra were observed in the frequency regions of the carboxylic and carboxylate groups. Residues were identified by [4-^{13}C] isotopic labeling of Asp residues[26-27] and mutational studies.[28-32] These studies clarified that Asp85 and Asp96 change their protonation states during the photocycle. Asp85 is deprotonated in the unphotolyzed state, becomes protonated in the L-to-M transition, and is again deprotonated in the O-to-unphotolyzed state transition. Asp96 is protonated in the unphotolyzed state, becomes deprotonated in the M-to-N transition, and is reprotonated in the N-to-O transition. Figure 3A summarizes the proton-transporting mechanism of *Hs*BR. Acid dissociation constants were determined for the proton relay points,[33-35] which are consistent with the proposed proton transfer in the photocycle. Another key element of the proton-pumping rhodopsins, water molecules bound in the protein, was also studied by IR spectroscopy.[36-39]

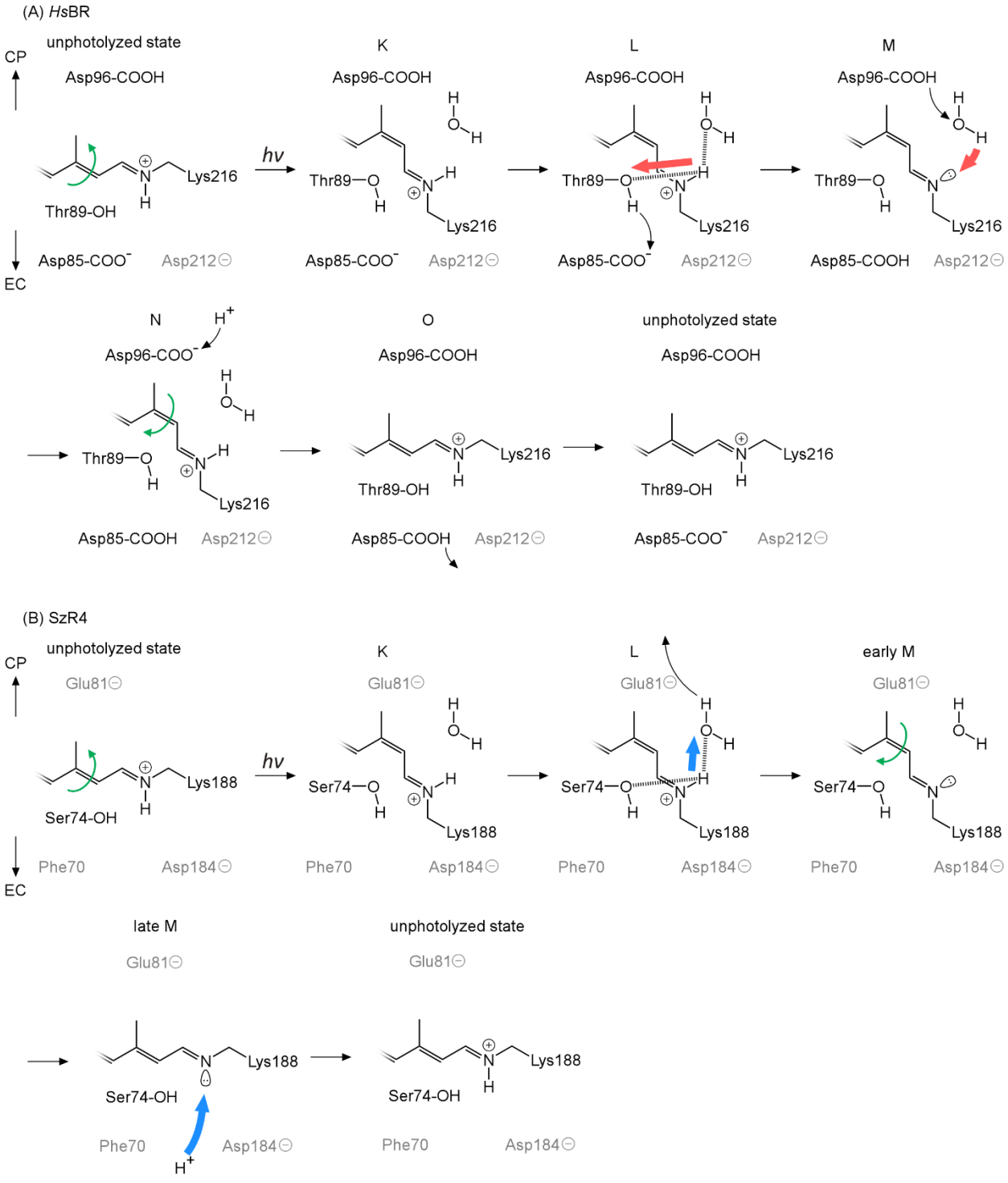

Figure 3. Diagrams illustrating the structural alternations in the retinal chromophore and proton movement in the photocycles of *Hs*BR (A) and SzR4 (B). The top and bottom portions of each diagram represent the cytoplasmic and extracellular regions, respectively.

3. Proton-Transporting Mechanism of Schizorhodopsins: Inward Proton Pump

Here, we describe insights obtained from our time-resolved RR studies on SzR4. Although crystallographic data of SzR4 are available for the unphotolyzed state,[40] no crystallographic data were reported for the intermediates. The RR spectra provided conclusive information on the structure of the retinal chromophore in the intermediates, thereby elucidating the inward proton-pumping mechanism and factors determining the proton transport direction of SzRs.

Figure 4 displays the RR spectra of SzR4 in its unphotolyzed state, measured at 532 nm in H_2O (A) and D_2O (B) buffer, shown in trace a. The observed spectral characteristics closely resembled those of light-adapted *Hs*BR. We identified the Raman bands of SzR4 based on previous vibrational analysis of light-adapted *Hs*BR. The C=N stretching [ν(C=N)] mode of the Schiff base, formed by retinal and Lys188 residue, was attributed to a band at 1638 cm^{-1}. A prominent band at 1525 cm^{-1} was assigned to the in-phase ethylenic C=C stretching [ν(C=C)] mode, with less intense bands at 1546, 1576, and 1596 cm^{-1} corresponding to out-of-phase ν(C=C) modes. Hydrogen deformation of the methyl groups on C_9 and C_{13} atoms produced bands at 1378, 1443, and 1472 cm^{-1}. C–CH rocking bands were detected at 1269, 1302, and 1320 cm^{-1}, while the C–NH rocking band was observed at 1352 cm^{-1}. Bands in the range of 1162–1241 cm^{-1} were associated with skeletal C–C stretching [ν(C–C)] modes. Rocking modes of the methyl groups was observed at 1005 cm^{-1}. Lastly, bands between 878–987 cm^{-1} were assigned to hydrogen-out-of-plane (HOOP) wagging modes.

We conducted time-resolved RR measurements on intermediates appearing in the photocycle of SzR4. The observed time-resolved RR spectra contained contributions from several intermediates, which is illustrated in Figure 2B. We decomposed the observed time-resolved RR spectra into the spectra of the individual intermediates, which are shown in Figure 4.

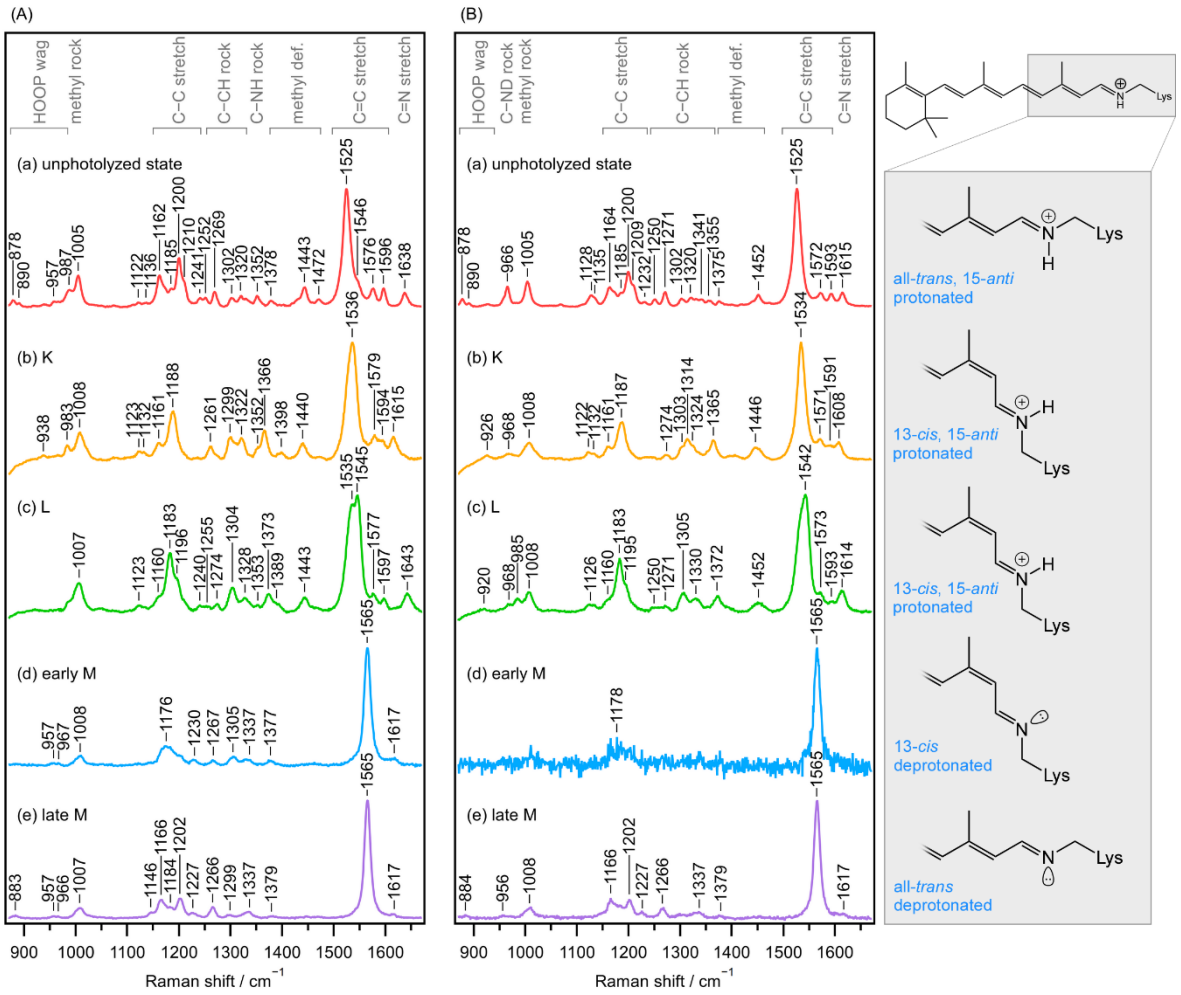

Figure 4. RR spectra of SzR4 in H_2O (A) and D_2O (B) buffers. The wavelengths of the probe light were 532, 475, 475, 405, and 405 nm for the unphotolyzed state (a), K (b), L (c), early M (d), and late M intermediates (e), respectively. The photoreaction was initiated by 532-nm excitation.

Assignments of spectral components observed in the time-resolved spectra were made based on the time constants obtained by transient absorption spectroscopy.[40] Traces b and c were obtained from the time-resolved spectra measured with 532-nm pump and 475-nm probe lights. Traces d and e were obtained from the time-resolved spectra measured with 532-nm pump and 405-nm probe lights. The wavelengths of the probe light were selected such that Raman scattering due to

the intermediate of interest was resonantly enhanced. Two spectral components attributable to the M intermediates were observed at 0.1–15 ms, which were designated as early and late M intermediates since the two intermediates appeared sequentially. The RR spectra of the intermediates exhibited different features from each other, showing structural evolutions in the photocycle. Structures of the intermediates of SzR4 are discussed in the following sections.

3-1. Protonation State of the Schiff Base in SzR4

Deuteration effects on RR spectra of the retinal chromophore provide information on the protonation state at the Schiff base in the retinal chromophore because the Schiff base is the sole site to which a proton can be bound. In the spectra of the unphotolyzed state, the ν(C=N) band at 1638 cm^{-1} was downshifted to 1615 cm^{-1} upon deuteration. This downshift is because the ν(C=N) vibration is coupled with the C–NH rocking vibration of the Schiff base. In addition, the C–NH rocking bands at 1352 cm^{-1} in H_2O buffer disappeared in the spectra measured in D_2O and an additional band was observed at 966 cm^{-1} arising from the C–ND rocking mode. The deuteration shifts of the ν(C=N) and C–NH rocking bands are useful markers of the protonation state of the Schiff base. These observations indicate that the Schiff base is protonated in the unphotolyzed state of SzR4, as in other ion-pumping rhodopsins.

Deuteration shifts of the ν(C=N) band were also observed in the spectra of the K and L intermediates. Conversely, the spectra of the late M intermediates showed no observable shifts.[41] These results indicate that the Schiff base becomes deprotonated during the L-to-M transition and is reprotonated upon recovery from the late M intermediate to the unphotolyzed state, consistent with conclusions derived from transient absorption measurements.[40]

3-2. Isomerization Site of the Retinal Chromophore in SzR4

The ν(C–C) band frequencies and intensities are highly responsive to retinal chromophore configurations, as polyene chain arrangements influence bond order and vibrational coupling.[42] In the unphotolyzed state, strong ν(C–C) bands were detected at 1162 and 1200 cm^{-1}, corresponding to C_{10}–C_{11} and C_{14}–C_{15} stretching modes, respectively. These intensities indicate the C_{13}=C_{14} configuration of the retinal chromophore.[21-22] The spectral characteristics resemble those of light-adapted *Hs*BR, where the retinal chromophore adopts an all-*trans* configuration, suggesting that the retinal chromophore of SzR4 also adopts the all-*trans* form in the unphotolyzed state. The 1200 cm^{-1} band in the H_2O buffer spectrum is attributed to the C_{14}–C_{15} stretching mode in the all-*trans* configuration, which is affected by the C_{15}=N configuration.[43] The D_2O buffer spectrum showed no deuteration effect on the 1200 cm^{-1} band, similar to light-adapted *Hs*BR, indicating a *trans* configuration of the C_{15}=N bond (15-*anti* configuration). These configuration assignments align with X-ray crystallographic data.[40] The ν(C–C) band features demonstrate that the retinal chromophore in the unphotolyzed state adopts an all-*trans* and 15-*anti* configuration. Comparable characteristics were observed in other SzRs.[1, 4]

The K and L intermediates exhibited strong ν(C–C) bands at 1188 and 1183 cm^{-1}, respectively, which were completely different from those for the unphotolyzed state. No deuteration shift was observed for the ν(C–C) bands. These features are similar to those observed for the K and L intermediates of *Hs*BR, in which the retinal chromophore adopts the 13-*cis* and 15-*anti* configurations.[22, 44-47] This similarity shows that the chromophore undergoes isomerization from the all-*trans* to the 13-*cis* configuration in SzR4 upon photoexcitation.

A notable contrast was observed in the spectral characteristics of the ν(C–C) bands between 1150–1250 cm^{-1} for the two M intermediates, indicating a difference in their configurations. The

early M intermediate displayed a strong band at 1176 cm^{-1} in the ν(C−C) region, which is indicative of the 13-*cis* configuration.[22, 44-47] In contrast, the late M intermediate showed two distinct ν(C−C) bands at 1166 and 1202 cm^{-1}, along with a pronounced C−CH rocking band at 1266 cm^{-1}. Remarkably, these spectral features of the late M intermediate do not resemble any of those for other M intermediates of ion-pumping rhodopsins. The features of the ν(C−C) and C−CH rocking bands of the late M intermediate resembled those of the authentic deprotonated all-*trans* retinal chromophores, providing strong evidence that the chromophore of the late M intermediate is in the all-*trans* configuration. Consequently, it can be concluded that the SzR4 chromophore undergoes reisomerization prior to the reprotonation of the Schiff base.

In SzR4, we noted a unique series of structural alterations in the retinal chromophore, where *cis–trans* reisomerization occurs before reprotonation. This contrasts with all previously reported photocycles for proton-pumping rhodopsins, where *cis–trans* reisomerization follows the reprotonation of the chromophore's Schiff base.[6] *Cis–trans* reisomerization following reprotonation was also noted for sodium ion-pumping rhodopsins[48-49] and heliorhodopsins.[50] Therefore, reisomerization preceding reprotonation is a unique characteristic of SzR4 in ion-pumping rhodopsins revealed in our study. This feature was also observed for the M intermediates of SzRs other than SzR4.[1, 4] Our finding for SzRs has discovered a critical counterexample to the generally accepted rule in the proton-pumping rhodopsins.

3-3. Facilitation of Thermal Reisomerization in SzR4

The deprotonated chromophore exhibits stronger bond alternation compared to its protonated counterpart,[42] suggesting a slower *thermal cis–trans* isomerization process for the former, unless the effect of opsin is considered. However, despite the C_{13}=C_{14} bond having a higher bond order, SzRs demonstrate thermal *cis–trans* isomerization rates that are similar to or exceed those of

outward proton-pumping rhodopsins.[51-53] This indicates that in SzRs, the opsin must play a role in facilitating the thermal *cis–trans* isomerization process.

High atomic packing is typically crucial for facilitating the propagation of subsequent structural changes to spatially distinct locations.[54-55] In our previous work, we have highlighted the essential roles of close atomic interactions between the retinal chromophore and its adjacent amino acids in ion-pumping rhodopsins.[56-57] Atomic contacts of the retinal chromophore to neighboring residues around the C_{13}=C_{14} bond in SzR4 are tighter than those in *Hs*BR, as evidenced by unusually intense HOOP bands in the unphotolyzed state.[1] Additionally, our findings demonstrated a correlation between HOOP intensities and the rate of *cis–trans* reisomerization.[4] This relationship indicates that close atomic interactions destabilize the 13-*cis* configuration due to steric effects, facilitating rapid thermal reisomerization, even when the order of the C_{13}=C_{14} bond is high in the deprotonated chromophore.

3-4. Hydrogen-Bonding Strength and Partners of the Schiff Base in SzR4

The deuteration effect on the ν(C=N) band provides information not only on the protonation state of the Schiff base but also the hydrogen-bonding strength of the protonated Schiff base.[58] The magnitude of the deuteration shift was 23 cm^{-1} for the unphotolyzed state, indicating the presence of a strong hydrogen bond at the protonated Schiff base. Furthermore, the bandwidth of the ν(C=N) band provides information on the hydrogen-bonding partner of the Schiff base.[59] The ν(C=N) band is broadened when a water molecule is located close to the Schiff base due to the energy transfer between the ν(C=N) mode of the Schiff base and the bending mode of the water molecule. The broadening of the ν(C=N) band was not observed for the unphotolyzed state, providing experimental support for the lack of water molecule proximity to the protonated Schiff

base in SzR4, in sharp contrast to *Hs*BR, in which a water molecule is hydrogen-bonded to the protonated Schiff base (Figure 5A and 5B).

The deuteration shifts of the ν(C=N) band are 7 and 29 cm^{-1} for the K and L intermediates, respectively, showing that the hydrogen bond of the protonated Schiff base experiences a reduction in strength in the K intermediate, whereas it becomes stronger in the L intermediate than in the unphotolyzed state. The strengthening of the hydrogen bond is advantageous for the subsequent proton release from the Schiff base in the subsequent step to the M intermediates because it lowers the barrier height for proton dissociation. In contrast to the unphotolyzed state, broadening of the ν(C=N) band in H_2O buffer was observed in the RR spectrum of the L intermediates, showing that the Schiff base forms a strong hydrogen bond to a water molecule in the L intermediate of SzR4.[60] The large deuteration shift and broadening of the ν(C=N) band

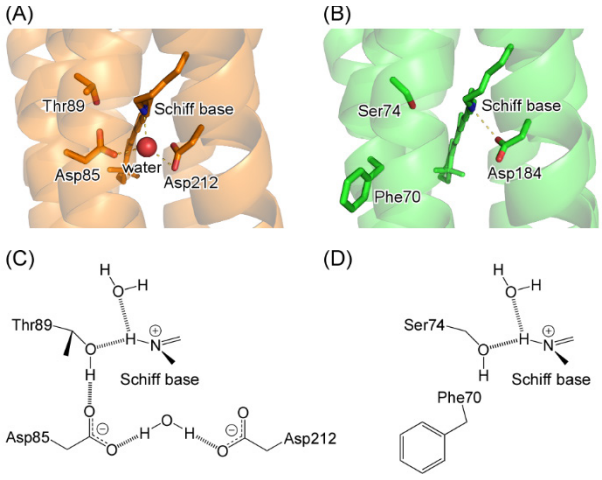

Figure 5. Structures around the Schiff base in *Hs*BR and SzR4. Upper panels compare crystal structures for the unphotolyzed states of *Hs*BR (A, PDB ID: 1C3W) and SzR4 (B, PDB ID: 7E4G). The red sphere in panel A represents the oxygen atom of the internal water molecule. Yellow dashed lines show hydrogen bonds. Lower panels show structures of hydrogen bonding networks for protonated Schiff base in L intermediates of *Hs*BR (C) and SzR4 (D).

were also observed for the L intermediate of *Hs*BR.[61-63] Time-resolved crystallographic studies revealed that the protonated Schiff base is hydrogen-bonded to the hydroxy group of Thr89 and a water molecule in the L intermediate of *Hs*BR (Figure 5C).[64-65] In SzR4, Ser74 is located in the position corresponding to Thr89 in *Hs*BR. Our observation suggests that the protonated Schiff base of SzR4 is bonded in the same fashion as that for *Hs*BR; it is hydrogen-bonded to the hydroxy group of Ser74 and a water molecule in the L intermediate of SzR4 (Figure 5D).[60] Although the strong hydrogen bond of the Schiff base, which likely facilitates proton dissociation from the Schiff base, is common for the L intermediates of both pumps, the movement of the dissociated proton differed between the two pumps. Because no structural difference responsible for the direction difference of the proton transfer was observed in the Schiff base of the L intermediate, the direction must be determined by the environment of the Schiff base. It is highly likely that the difference in the direction of the proton transfer arises from the number of negative charges located on the extracellular side of the Schiff base. Two Asp residues are positioned on the extracellular side of the Schiff base in *Hs*BR and other outward proton-pumping rhodopsins (Figure 5A). In contrast, in SzRs, the corresponding Asp residue in helix C is replaced with a Phe or Tyr residue, resulting in a single negative charge on the extracellular side (Figure 5B). The two Asp residues in *Hs*BR form a strongly attractive electrostatic field for the dissociated proton, enabling proton transfer across the retinal chromophore. This is also consistent with the experimental fact that replacing Asp212 prevented the proton release by the Schiff base even though the proton acceptor (Asp85) and the proton donor (Asp96) for the Schiff base were unreplaced in *Hs*BR.[66-67] The presence of a strongly hydrogen-bonded water molecule was revealed for the unphotolyzed state of outward proton-pumping rhodopsins.[37, 68] The water molecule is likely located between the two Asp residues,

which are conserved residues in outward proton-pumping rhodopsins. The presence of the strongly hydrogen-bonded water molecule is a reasonable consequence of a strong electrostatic field formed by the two negative charges of the Asp residues. In contrast, in SzR4, the attractive electrostatic field is weak enough for the dissociated proton to move toward the cytoplasmic media. Replacement of Asp184 with an Asn residue resulted in the loss of both the color of the protein and proton-transporting activity in SzR4, indicating that deprotonation of the Schiff base occurred.[40] Thus, the negative charge on Asp184 stabilizes protonation at the Schiff base but does not attract the dissociated proton to the extracellular side of the retinal chromophore, resulting in proton release toward the cytoplasmic medium in the early M intermediate.

4. Comparison of the Proton-Pumping Mechanisms of SzR4 and *Hs*BR

Comparing structural changes of the retinal chromophores of SzR4 and *Hs*BR will deepen our understanding of their proton-pumping mechanisms. Their structural changes are summarized in Figure 3. Our attention was directed towards the alignment of the N−H group and the nitrogen atom's lone pair within the Schiff base, as these elements play a critical role in determining the directionality of proton transport. In *Hs*BR, the chromophore adopts the all-*trans* configuration in the unphotolyzed state. The photoexcitation induces the isomerization to the 13-*cis* form, accompanied by the reorientation of the N−H group towards the cytoplasmic side (Figure 3A, K and L intermediates). This configuration is unfavorable for proton transfer from the Schiff base to Asp85, the proton acceptor situated on the extracellular side of the Schiff base. Nevertheless, during the L-to-M transition, the proton is transferred from the Schiff base to Asp85 due to the strong attractive electrostatic field created by the two negative charges on Asp85 and Asp212. Subsequently, in the M-to-N transition, the nitrogen atom's lone pair at the Schiff base, which continues to face the cytoplasmic side, accepts a proton from Asp96, the proton donor located on

the cytoplasmic side of the Schiff base.[29, 31, 69-70] Conversely, in SzR4, the presence of only one Asp residue near the Schiff base results in an insufficient attractive electrostatic field to move the released proton towards the extracellular side of the Schiff base (Figure 3B). As a result, the proton that dissociates from the Schiff base is transported to the solvent through a water-mediated network, drawn by the negative charge of Glu81,[16] which is homologous to Asp96 in *Hs*BR. While the E81Q mutant of SzR4 lost the proton-pumping activity,[40] E81Q mutation for AntR, a member of the SzR subgroup within microbial rhodopsins, did not affect inward proton-pumping efficiency and accelerated the formation of the M intermediate.[19]

The retinal chromophore is thermally isomerized from 13-*cis* to all-*trans* configuration during the early M-to-late M transition in SzRs including SzR4.[3] This isomerization shifts the nitrogen lone pair from the cytoplasmic to the extracellular side, facilitating the deprotonated Schiff base in accepting a proton from the extracellular environment. The retinal chromophore of *Po*XeR changes from the 13-*cis* and 15-*anti* forms to the 13-*cis* and 15-*syn* forms, causing the nitrogen lone pair to point towards the extracellular side and then undergo the 13-*cis*-to-*trans* and 15-*syn*-to-*anti* dual thermal isomerization to return to its original configuration.[16] Intriguingly, SzR4 adopts a simpler mechanism to redirect the nitrogen lone pair towards the extracellular side by reversing the order of C_{13}=C_{14} reisomerization and reprotonation.

5. Mechanism of Unidirectional Proton Transfer

Unidirectional proton transfer is generally based on concerted changes in the proton affinities at the transient proton-binding sites in the proteins,[71] which, may not be necessary for inward proton pumping of SzRs. In SzR4, the N–H group in the L intermediate faces the cytoplasmic side, while the nitrogen lone pair at the Schiff base in the late M intermediate is oriented towards the extracellular side (Figure 3B). These orientations correspond to the directions of proton

release and uptake for inward proton transport. Unidirectional proton transport becomes feasible without transient proton-binding residues when the acid dissociation constant for the Schiff base is higher in the all-*trans* configuration and lower in the 13-*cis* configuration compared to aqueous media. This is achieved through configurational changes-induced protonation/deprotonation switching in the Schiff base.[3] The absence of identified transient proton-accepting or donating residues in SzRs[20] suggests that protons are transferred via the water-mediated network, including a negatively charged residue,[40, 72-73] through Grotthuss-type proton migration. The lack of a proton-donating residue to the Schiff base in SzRs may decelerate reprotonation in the late M intermediate, allowing *cis–trans* isomerization to occur before reprotonation. In contrast, outward proton-pumping rhodopsins require transient proton-binding residues and concerted changes in proton affinities at these sites, as the proton released from the Schiff base must be accepted by an amino acid residue on the extracellular side of the Schiff base.[71] The simplicity and rationality of the SzR proton-pumping mechanism make it valuable for designing artificial proton-transporting molecular systems.[74-75]

6. Protonated Schiff Base: Steering the Ion Transfer in Ion-pumping Rhodopsins

We evaluated the direction of the N–H group of the protonated Schiff base and the lone pair of the deprotonated Schiff base in the inward and outward proton-pumping rhodopsins. The N–H group direction and hydrogen bonding strength of the protonated Schiff base are also essential to other ion-pumping mechanisms. The hydrogen bonding strength is correlated with the ion-transporting function. Table 1 summarizes the ν(C=N) frequencies of ion-pumping rhodopsins in H_2O and D_2O. The chloride ion pumps show the smallest frequency differences upon deuteration, followed by the outward proton pumps, while the outward sodium ion and inward proton pumps show the largest frequency differences.

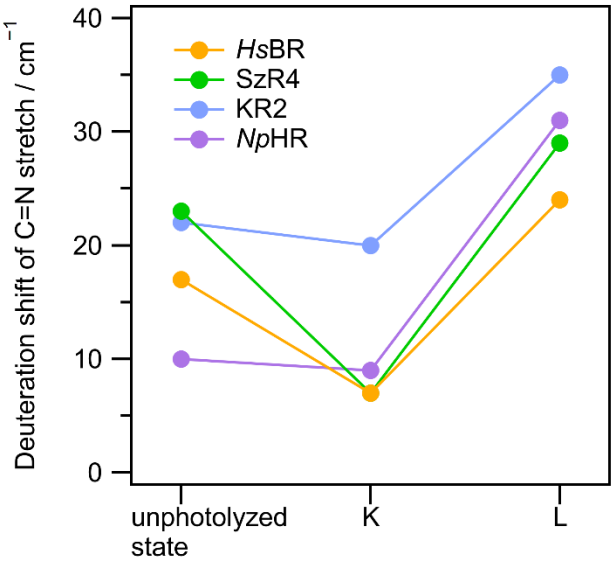

Figure 6. Evolutions of the ν(C=N) deuteration shifts from the unphotolyzed state to primary intermediates of SzR4, *Hs*BR, *Np*HR, and KR2.

We found that both the outward and inward proton pumps have a strong hydrogen bond at the Schiff base in the L intermediate. Interestingly, a strong hydrogen bond at the Schiff bases in the L intermediate was observed in the chloride ion- and sodium ion-pumping rhodopsins as well. Figure 6 shows the transitions of the ν(C=N) frequency differences of SzR4, *Hs*BR, halorhodopsin from *Natronomonas pharaonis* (*Np*HR), which is a representative chloride ion pump, and *Krokinobacter* rhodopsin 2 (KR2), which is a representative sodium ion pump. The following reasons for the strong hydrogen bond of the L intermediate are proposed. In sodium-ion-pumping rhodopsin, sodium ions are transported through the vicinity of the Schiff base. To avoid electrostatic repulsion with sodium ions, the Schiff base must be deprotonated when sodium ions pass through it. For this reason, the activation barrier for the deprotonation of the Schiff base must be lowered in the L intermediate, as in proton-pumping rhodopsins. In chloride-ion-pumping rhodopsins, chloride ions are drawn to the positive charge of the protonated Schiff

base to move from the extracellular to the intracellular side of the retinal chromophore in the L intermediate. For this purpose, it is advantageous that the N–H bond of the protonated Schiff base is strongly polarized. Accordingly, for all ion pumps, the strong hydrogen bonding of the Schiff base in the L intermediate is advantageous for their ion-transporting functions. Even more interestingly, the position of the hydrogen bonding partner of the Schiff base is similar between the proton-pumping and sodium ion-pumping rhodopsins. We have already described that, in the L intermediate, the protonated Schiff base is hydrogen-bonded to a hydroxy-bearing residue, which is located in a position common to the inward (Ser74 in SzR4) and outward proton-pumping rhodopsins (Thr89 in *Hs*BR). In KR2, the protonated Schiff base forms a hydrogen bond to Asp116 (corresponding to Thr89 in *Hs*BR and Ser74 in SzR4) in the L intermediate.[76] In the chloride ion-pumping rhodopsin (*Nonlabens marinus* halorhodopsin), the protonated Schiff base interacts with Thr102 (corresponding to Thr89 in *Hs*BR and Ser74 in SzR4) via a chloride ion.[77]

Table 1. C=N Stretching Frequencies of the Protonated Schiff Base for the Unphotolyzed State of Ion-Pumping Rhodopsins.

Protein	ν(C=N) / cm^{-1}		Δν(C=N) / cm^{-1}	Ref.
	In H_2O	In D_2O		
Inward proton pump				
SzR1	1638	1615	23	1
SzR2	1643	1619	24	1
SzR3	1646	1619	27	1
SzR4	1638	1615	23	1
*Ms*SzR	1644.1	1619.6	24.5	4
*Mt*SzR	1643.4	1617.5	25.9	4
AntR	1640.4	1617.8	22.6	4
Outward proton pump				
*Hs*BR	1640	1624	16	21
*Hs*BR	1642	1624	18	78
*Hs*BR	1642	1625	17	46
Archaerhodopsin 3	1641	1621	20	79
Thermophilic rhodopsin	1640	1625	15	80
Blue-light-absorbing proteorhodopsin	1657	1636	21	81
Green-light-absorbing proteorhodopsin	1654	1631	23	81
Gloeobacter rhodopsin	1639	1625	14	60
Chloride ion pump				
*Hs*HR	1633	1621	12	82
*Hs*HR	1635	1623	12	83
*Hs*HR	1632	1621	11	84
*Np*HR	1632	1622	10	85
*Np*HR	1633	1622	11	86
Sodium ion pump				
KR2	1640	1618	22	48
*Ia*NaR	1644	1622	22	87
*Be*NaR	1642	1620	22	88

7. Summary and Outlook

In this Account, we present insights obtained by our recent studies on inward proton-pumping rhodopsins. The revealed chromophore structures of their intermediates well explain the unidirectional proton-pumping mechanism, suggesting a simpler proton-transporting mechanism for SzRs than that for other proton-pumping rhodopsins. The Schiff base is the key to determining the transport direction. The structure of the Schiff base was further discussed by extending the comparison to chloride ion-pumping and sodium ion-pumping rhodopsins.

Many ion-pumping rhodopsins have been discovered in the last quarter of a century, which increased the variety of ion-pumping rhodopsins in terms of structure and function.[14-15] Therefore, a basis for understanding the amino acid sequence-structure-function relationship was established by comparing these ion-pumping rhodopsins. Functional conversion by amino acid substitution is a straightforward approach for examining the sequence-structure-function relationships.[89-92] Another effective and emerging approach is to study ancestral proteins from which sequences are derived by ancestral sequence reconstruction.[93-95] In addition to swapping residues between homologous proteins of extant species (horizontal comparison), which may not be evolutionarily relevant, an alternative vertical approach, which is to trace sequence modifications through the evolution of genomes and species, will advance our understanding of the amino acid sequence-structure-function relationships of proteins. Ancestral sequence reconstruction has been applied to predict sequences of ancestral ion-pumping rhodopsins.[96] Further improvements in the accuracy of the prediction will accelerate understanding of the sequence-structure-function relationships of ion-pumping rhodopsins.

Biography

Taito Urui

Taito Urui received his B.S. in 2020 and earned his M.S. in 2022 from Osaka University mentored by Professor Yasuhisa Mizutani. His Ph.D. research at Osaka University focuses on elucidation of functional mechanisms of microbial rhodopsins.

Yasuhisa Mizutani

Yasuhisa Mizutani earned his B.E. from Kyoto University in 1987 and his Ph.D. from the Graduate University for Advanced Studies in 1992. After postdoctoral research at the University of Pennsylvania and the Institute for Molecular Science, he started as a research associate at the Institute for Molecular Science in 1994. He became an associate professor at Kobe University in 2001 and a full professor at Osaka University in 2006. Mizutani's research focuses on using time-resolved RR spectroscopy to study protein dynamics and energetics essential for their function.

AUTHOR INFORMATION

Corresponding Author

Yasuhisa Mizutani — *Department of Chemistry, Graduate School of Science, Osaka University, 1-1 Machikaneyama, Toyonaka, Osaka 560-0043, Japan*; orcid.org/0000-0002-3754-5720; Email: mztn@chem.sci.osaka-u.ac.jp; Tel: +81-6-6850-5776.

Notes

The authors declare no competing financial interests.

ACKNOWLEDGMENT

This Account reflects the collective efforts of both past and present collaboration partners whose names can be found in the cited references. We extend our heartfelt thanks to all of them. This material is based on work supported by Grants-in-Aid from the JSPS (JP22J22606, T.U.; JP20H02693, Y.M.; JP23H00285, Y.M.).

REFERENCES

1. Shionoya, T.; Singh, M.; Mizuno, M.; Kandori, H.; Mizutani, Y., Strongly Hydrogen-Bonded Schiff Base and Adjoining Polyene Twisting in the Retinal Chromophore of Schizorhodopsins. *Biochemistry* **2021,** *60*, 3050-3057.
2. Hayashi, K.; Mizuno, M.; Kandori, H.; Mizutani, Y., *Cis–Trans* Reisomerization Precedes Reprotonation of the Retinal Chromophore in the Photocycle of Schizorhodopsin 4. *Angew. Chem. Int. Ed.* **2022,** *61*, e202203149.
3. Urui, T.; Hayashi, K.; Mizuno, M.; Inoue, K.; Kandori, H.; Mizutani, Y., *Cis–Trans* Reisomerization Preceding Reprotonation of the Retinal Chromophore Is Common to the Schizorhodopsin Family: A Simple and Rational Mechanism for Inward Proton Pumping. *J. Phys. Chem. B* **2024,** *128*, 744-754.
4. Urui, T.; Shionoya, T.; Mizuno, M.; Inoue, K.; Kandori, H.; Mizutani, Y., Chromophore–Protein Interactions Affecting the Polyene Twist and π–π* Energy Gap of the Retinal Chromophore in Schizorhodopsins. *J. Phys. Chem. B* **2024,** *128*, 2389-2397.
5. Stein, W. D.; Litman, T., *Channels, Carriers, and Pumps*. second ed.; Academic Press: London, 2015.
6. Ernst, O. P.; Lodowski, D. T.; Elstner, M.; Hegemann, P.; Brown, L. S.; Kandori, H., Microbial and Animal Rhodopsins: Structures, Functions, and Molecular Mechanisms. *Chem. Rev.* **2014,** *114*, 126-163.
7. Inoue, K., Photochemistry of the Retinal Chromophore in Microbial Rhodopsins. *J. Phys. Chem. B* **2023,** *127*, 9215-9222.
8. Oesterhelt, D.; Stoeckenius, W., Rhodopsin-Like Protein from the Purple Membrane of *Halobacterium Halobium*. *Nature New Biol.* **1971,** *233*, 149-152.
9. Blaurock, A. E.; Stoeckenius, W., Structure of the Purple Membrane. *Nature New Biol.* **1971,** *233*, 152-155.
10. Matsuno-Yagi, A.; Mukohata, Y., Two Possible Roles of Bacteriorhodopsin; a Comparative Study of Strains of Halobacterium Halobium Differing in Pigmentation. *Biochem. Biophys. Res. Commun.* **1977,** *78*, 237-243.
11. Schobert, B.; Lanyi, J. K., Halorhodopsin Is a Light-Driven Chloride Pump. *J. Biol. Chem.* **1982,** *257*, 10306-13.
12. Inoue, K.; Ono, H.; Abe-Yoshizumi, R.; Yoshizawa, S.; Ito, H.; Kogure, K.; Kandori, H., A Light-Driven Sodium Ion Pump in Marine Bacteria. *Nat. Commun.* **2013,** *4*, 1678.
13. Kwon, S.-K.; Kim, B. K.; Song, J. Y.; Kwak, M.-J.; Lee, C. H.; Yoon, J.-H.; Oh, T. K.; Kim, J. F., Genomic Makeup of the Marine Flavobacterium *Nonlabens* (*Donghaeana*) *Dokdonensis* and Identification of a Novel Class of Rhodopsins. *Genome Biology and Evolution* **2013,** *5*, 187-199.
14. Govorunova, E. G.; Sineshchekov, O. A.; Li, H.; Spudich, J. L., Microbial Rhodopsins: Diversity, Mechanisms, and Optogenetic Applications. *Annu. Rev. Biochem.* **2017,** *86*, 845-872.
15. Rozenberg, A.; Inoue, K.; Kandori, H.; Béjà, O., Microbial Rhodopsins: The Last Two Decades. *Annu. Rev. Microbiol.* **2021,** *75*, 427-447.
16. Inoue, K.; Ito, S.; Kato, Y.; Nomura, Y.; Shibata, M.; Uchihashi, T.; Tsunoda, S. P.; Kandori, H., A Natural Light-Driven Inward Proton Pump. *Nat. Commun.* **2016,** *7*, 13415.
17. Bulzu, P.-A.; Andrei, A.-Ş.; Salcher, M. M.; Mehrshad, M.; Inoue, K.; Kandori, H.; Beja, O.; Ghai, R.; Banciu, H. L., Casting Light on Asgardarchaeota Metabolism in a Sunlit Microoxic Niche. *Nature Microbiol.* **2019,** *4*, 1129-1137.

18. Kawasaki, Y.; Konno, M.; Inoue, K., Thermostable Light-Driven Inward Proton Pump Rhodopsins. *Chem. Phys. Lett.* **2021,** *779*, 138868.
19. Harris, A.; Lazaratos, M.; Siemers, M.; Watt, E.; Hoang, A.; Tomida, S.; Schubert, L.; Saita, M.; Heberle, J.; Furutani, Y., et al., Mechanism of Inward Proton Transport in an Antarctic Microbial Rhodopsin. *J. Phys. Chem. B* **2020,** *124*, 4851-4872.
20. Inoue, K.; Tsunoda, S. P.; Singh, M.; Tomida, S.; Hososhima, S.; Konno, M.; Nakamura, R.; Watanabe, H.; Bulzu, P.-A.; Banciu, H. L., et al., Schizorhodopsins: A Family of Rhodopsins from Asgard Archaea That Function as Light-Driven Inward H^+ Pumps. *Sci. Adv.* **2020,** *6*, eaaz2441.
21. Smith, S. O.; Braiman, M. S.; Myers, A. B.; Pardoen, J. A.; Courtin, J. M. L.; Winkel, C.; Lugtenburg, J.; Mathies, R. A., Vibrational Analysis of the All-*trans*-Retinal Chromophore in Light-Adapted Bacteriorhodopsin. *J. Am. Chem. Soc.* **1987,** *109*, 3108-3125.
22. Smith, S. O.; Pardoen, J. A.; Lugtenburg, J.; Mathies, R. A., Vibrational Analysis of the 13-*cis*-Retinal Chromophore in Dark-Adapted Bacteriorhodopsin. *J. Phys. Chem.* **1987,** *91*, 804-819.
23. Aton, B.; Doukas, A. G.; Callender, R. H.; Becher, B.; Ebrey, T. G., Resonance Raman Studies of the Purple Membrane. *Biochemistry* **1977,** *16*, 2995-2999.
24. Rothschild, K. J.; Zagaeski, M.; Cantore, W. A., Conformational Changes of Bacteriorhodopsin Detected by Fourier Transform Infrared Difference Spectroscopy. *Biochem. Biophys. Res. Commun.* **1981,** *103*, 483-489.
25. Siebert, F.; Mäntele, W.; Kreutz, W., Evidence for the Protonation of Two Internal Carboxylic Groups During the Photocycle of Bacteriorhodopsin. *FEBS Letters* **1982,** *141*, 82-87.
26. Engelhard, M.; Gerwert, K.; Hess, B.; Kreutz, W.; Siebert, F., Light-Driven Protonation Changes of Internal Aspartic Acids of Bacteriorhodopsin: An Investigation by Static and Time-Resolved Infrared Difference Spectroscopy Using [4-^{13}C]Aspartic Acid Labeled Purple Membrane. *Biochemistry* **1985,** *24*, 400-7.
27. Eisenstein, L.; Lin, S. L.; Dollinger, G.; Odashima, K.; Termini, J.; Konno, K.; Ding, W. D.; Nakanishi, K., FTIR Difference Studies on Apoproteins. Protonation States of Aspartic and Glutamic Acid Residues During the Photocycle of Bacteriorhodopsin. *J. Am. Chem. Soc.* **1987,** *109*, 6860-6862.
28. Braiman, M. S.; Mogi, T.; Marti, T.; Stern, L. J.; Khorana, H. G.; Rothschild, K. J., Vibrational Spectroscopy of Bacteriorhodopsin Mutants: Light-Driven Proton Transport Involves Protonation Changes of Aspartic Acid Residues 85, 96, and 212. *Biochemistry* **1988,** *27*, 8516-8520.
29. Braiman, M. S.; Bousché, O.; Rothschild, K. J., Protein Dynamics in the Bacteriorhodopsin Photocycle: Submillisecond Fourier Transform Infrared Spectra of the L, M, and N Photointermediates. *Proc. Natl. Acad. Sci. USA* **1991,** *88*, 2388-2392.
30. Gerwert, K.; Hess, B.; Soppa, J.; Oesterhelt, D., Role of Aspartate-96 in Proton Translocation by Bacteriorhodopsin. *Proc. Natl. Acad. Sci. USA* **1989,** *86*, 4943-4947.
31. Gerwert, K.; Souvignier, G.; Hess, B., Simultaneous Monitoring of Light-Induced Changes in Protein Side-Group Protonation, Chromophore Isomerization, and Backbone Motion of Bacteriorhodopsin by Time-Resolved Fourier-Transform Infrared Spectroscopy. *Proc. Natl. Acad. Sci. USA* **1990,** *87*, 9774-9778.
32. Sasaki, J.; Lanyi, J. K.; Needleman, R.; Yoshizawa, T.; Maeda, A., Complete Identification of C=O Stretching Vibrational Bands of Protonated Aspartic Acid Residues in the

Difference Infrared Spectra of M and N Intermediates Versus Bacteriorhodopsin. *Biochemistry* **1994,** *33*, 3178-3184.
33. Braiman, M. S.; Dioumaev, A. K.; Lewis, J. R., A Large Photolysis-Induced pK_a Increase of the Chromophore Counterion in Bacteriorhodopsin: Implications for Ion Transport Mechanisms of Retinal Proteins. *Biophys. J.* **1996,** *70*, 939-47.
34. Brown, L. S.; Lanyi, J. K., Determination of the Transiently Lowered pK_a of the Retinal Schiff Base During the Photocycle of Bacteriorhodopsin. *Proc. Natl. Acad. Sci. USA* **1996,** *93*, 1731-1734.
35. Zscherp, C.; Schlesinger, R.; Tittor, J.; Oesterhelt, D.; Heberle, J., *In Situ* Determination of Transient pK_a Changes of Internal Amino Acids of Bacteriorhodopsin by Using Time-Resolved Attenuated Total Reflection Fourier-Transform Infrared Spectroscopy. *Proc. Natl. Acad. Sci. USA* **1999,** *96*, 5498-5503.
36. Maeda, A.; Sasaki, J.; Shichida, Y.; Yoshizawa, T., Water Structural Changes in the Bacteriorhodopsin Photocycle: Analysis by Fourier Transform Infrared Spectroscopy. *Biochemistry* **1992,** *31*, 462-467.
37. Kandori, H., Role of Internal Water Molecules in Bacteriorhodopsin. *Biochim. Biophys. Acta* **2000,** *1460*, 177-191.
38. Maeda, A.; Morgan, J. E.; Gennis, R. B.; Ebrey, T. G., Water as a Cofactor in the Unidirectional Light-Driven Proton Transfer Steps in Bacteriorhodopsin. *Photochem. Photobiol.* **2006,** *82*, 1398-1405.
39. Gerwert, K.; Freier, E.; Wolf, S., The Role of Protein-Bound Water Molecules in Microbial Rhodopsins. *Biochim. Biophys. Acta* **2014,** *1837*, 606-613.
40. Higuchi, A.; Shihoya, W.; Konno, M.; Ikuta, T.; Kandori, H.; Inoue, K.; Nureki, O., Crystal Structure of Schizorhodopsin Reveals Mechanism of Inward Proton Pumping. *Proc. Natl. Acad. Sci. USA* **2021,** *118*, e2016328118.
41. Due to low accumlation of the early M intermediate of SzR4 in D_2O buffer, the ν(C=N) band was not detected. However, no deuteration shift was observed for the early M intermediates of other SzRs.
42. Mathies, R. A.; Smith, S. O.; Palings, I., Determination of Retinal Chromophore Structure in Rhodopsins. In *Biological Application of Raman Spectroscopy*, Spiro, T. G., Ed. John Wiley and Sons: New York, 1988; Vol. II, pp 59-108.
43. Smith, S. O.; Myers, A. B.; Pardoen, J. A.; Winkel, C.; Mulder, P. P. J.; Lugtenburg, J.; Mathies, R., Determination of Retinal Schiff Base Configuration in Bacteriorhodopsin. *Proc. Natl. Acad. Sci. USA* **1984,** *81*, 2055-2059.
44. Doig, S. J.; Reid, P. J.; Mathies, R. A., Picosecond Time-Resolved Resonance Raman Spectroscopy of Bacteriorhodopsin's J, K, and KL Intermediates. *J. Phys. Chem.* **1991,** *95*, 6372-6379.
45. Fodor, S. P.; Pollard, W. T.; Gebhard, R.; van den Berg, E. M.; Lugtenburg, J.; Mathies, R. A., Bacteriorhodopsin's L_{550} Intermediate Contains a C14-C15 S-*trans*-Retinal Chromophore. *Proc. Natl. Acad. Sci. USA* **1988,** *85*, 2156-2160.
46. Lohrmann, R.; Grieger, I.; Stockburger, M., Resonance Raman Studies on the Intermediate K-590 in the Photocycle of Bacteriorhodopsin. *J. Phys. Chem.* **1991,** *95*, 1993-2001.
47. Smith, S. O.; Lugtenburg, J.; Mathies, R. A., Determination of Retinal Chromophore Structure in Bacteriorhodopsin with Resonance Raman Spectroscopy. *J. Membr. Biol.* **1985,** *85*, 95-109.

48. Nishimura, N.; Mizuno, M.; Kandori, H.; Mizutani, Y., Distortion and a Strong Hydrogen Bond in the Retinal Chromophore Enable Sodium-Ion Transport by the Sodium-Ion Pump KR2. *J. Phys. Chem. B* **2019,** *123*, 3430-3440.
49. Kandori, H.; Inoue, K.; Tsunoda, S. P., Light-Driven Sodium-Pumping Rhodopsin: A New Concept of Active Transport. *Chem. Rev.* **2018,** *118*, 10646-10658.
50. Urui, T.; Mizuno, M.; Otomo, A.; Kandori, H.; Mizutani, Y., Resonance Raman Determination of Chromophore Structures of Heliorhodopsin Photointermediates. *J. Phys. Chem. B* **2021,** *125*, 7155-7162.
51. Dioumaev, A. K.; Brown, L. S.; Shih, J.; Spudich, E. N.; Spudich, J. L.; Lanyi, J. K., Proton Transfers in the Photochemical Reaction Cycle of Proteorhodopsin. *Biochemistry* **2002,** *41*, 5348-5358.
52. Miranda, M. R. M.; Choi, A. R.; Shi, L.; Bezerra, A. G.; Jung, K.-H.; Brown, L. S., The Photocycle and Proton Translocation Pathway in a Cyanobacterial Ion-Pumping Rhodopsin. *Biophys. J.* **2009,** *96*, 1471-1481.
53. Bamann, C.; Bamberg, E.; Wachtveitl, J.; Glaubitz, C., Proteorhodopsin. *Biochim. Biophys. Acta* **2014,** *1837*, 614-625.
54. Mizutani, Y., Time-Resolved Resonance Raman Spectroscopy and Application to Studies on Ultrafast Protein Dynamics. *Bull. Chem. Soc. Jpn.* **2017,** *90*, 1344-1371.
55. Richards, F. M., The Interpretation of Protein Structures: Total Volume, Group Volume Distributions and Packing Density. *J. Mol. Biol.* **1974,** *82*, 1-14.
56. Shionoya, T.; Mizuno, M.; Kandori, H.; Mizutani, Y., Contact-Mediated Retinal–Opsin Coupling Enables Proton Pumping in *Gloeobacter* Rhodopsin. *J. Phys. Chem. B* **2022,** *126*, 7857-7869.
57. Urui, T.; Das, I.; Mizuno, M.; Sheves, M.; Mizutani, Y., Origin of a Double-Band Feature in the Ethylenic C═C Stretching Modes of the Retinal Chromophore in Heliorhodopsins. *J. Phys. Chem. B* **2022,** *126*, 8680-8688.
58. Baasov, T.; Friedman, N.; Sheves, M., Factors Affecting the C=N Stretching in Protonated Retinal Schiff Base: A Model Study for Bacteriorhodopsin and Visual Pigments. *Biochemistry* **1987,** *26*, 3210-3217.
59. Hildebrandt, P.; Stockburger, M., Role of Water in Bacteriorhodopsin's Chromophore: Resonance Raman Study. *Biochemistry* **1984,** *23*, 5539-5548.
60. Urui, T.; Mizuno, M.; Kandori, H.; Mizutani, Y., Structural Evolution of Retinal Chromophore in Early Intermediates of Inward and Outward Proton-Pumping Rhodopsins. submitted for publication.
61. Alshutn, T.; Stockburger, M., Time‐Resolved Resonance Raman Studies on the Photochemical Cycle of Bacteriorhodopsin. *Photochem. Photobiol.* **1986,** *43*, 55-66.
62. Lohrmann, R.; Stockburger, M., Time-Resolved Resonance Raman Studies of Bacteriorhodopsin and Its Intermediates K_{590} and L_{550}: Biological Implications. *J. Raman Spectrosc.* **1992,** *23*, 575-583.
63. Althaus, T.; Eisfeld, W.; Lohrmann, R.; Stockburger, M., Application of Raman Spectroscopy to Retinal Proteins. *Isr. J. Chem.* **1995,** *35*, 227-251.
64. Nango, E.; Royant, A.; Kubo, M.; Nakane, T.; Wickstrand, C.; Kimura, T.; Tanaka, T.; Tono, K.; Song, C.; Tanaka, R., et al., A Three-Dimensional Movie of Structural Changes in Bacteriorhodopsin. *Science* **2016,** *354*, 1552-1557.
65. Borshchevskiy, V.; Kovalev, K.; Round, E.; Efremov, R.; Astashkin, R.; Bourenkov, G.; Bratanov, D.; Balandin, T.; Chizhov, I.; Baeken, C., et al., True-Atomic-Resolution Insights into

the Structure and Functional Role of Linear Chains and Low-Barrier Hydrogen Bonds in Proteins. *Nat. Struct. Mol. Biol.* **2022,** *29*, 440-450.
66. Cao, Y.; Varo, G.; Klinger, A. L.; Czajkowsky, D. M.; Braiman, M. S.; Needleman, R.; Lanyi, J. K., Proton Transfer from Asp-96 to the Bacteriorhodopsin Schiff Base Is Caused by a Decrease of the pK_a of Asp-96 Which Follows a Protein Backbone Conformational Change. *Biochemistry* **1993,** *32*, 1981-1990.
67. Needleman, R.; Chang, M.; Ni, B.; Váró, G.; Fornés, J.; White, S. H.; Lanyi, J. K., Properties of Asp212→Asn Bacteriorhodopsin Suggest That Asp212 and Asp85 Both Participate in a Counterion and Proton Acceptor Complex near the Schiff Base. *J. Biol. Chem.* **1991,** *266*, 11478-11484.
68. Kandori, H., Structure/Function Study of Photoreceptive Proteins by FTIR Spectroscopy. *Bull. Chem. Soc. Jpn.* **2020,** *93*, 904-926.
69. Bousché, O.; Braiman, M.; He, Y. W.; Marti, T.; Khorana, H. G.; Rothschild, K. J., Vibrational Spectroscopy of Bacteriorhodopsin Mutants. Evidence That Asp-96 Deprotonates During the M----N Transition. *J. Biol. Chem.* **1991,** *266*, 11063-7.
70. Pfefferle, J. M.; Maeda, A.; Sasaki, J.; Yoshizawa, T., Fourier Transform Infrared Study of the N Intermediate of Bacteriorhodopsin. *Biochemistry* **1991,** *30*, 6548-6556.
71. Mizutani, Y., Concerted Motions and Molecular Function: What Physical Chemistry We Can Learn from Light-Driven Ion-Pumping Rhodopsins. *J. Phys. Chem. B* **2021,** *125*, 11812-11819.
72. Nagle, J. F.; Tristram-Nagle, S., Hydrogen Bonded Chain Mechanisms for Proton Conduction and Proton Pumping. *J. Membr. Biol.* **1983,** *74*, 1-14.
73. Luecke, H.; Richter, H.-T.; Lanyi, J. K., Proton Transfer Pathways in Bacteriorhodopsin at 2.3 Angstrom Resolution. *Science* **1998,** *280*, 1934-1937.
74. Steinberg-Yfrach, G.; Liddell, P. A.; Hung, S.-C.; Moore, A. L.; Gust, D.; Moore, T. A., Conversion of Light Energy to Proton Potential in Liposomes by Artificial Photosynthetic Reaction Centres. *Nature* **1997,** *385*, 239-241.
75. Mei, T.; Zhang, H.; Xiao, K., Bioinspired Artificial Ion Pumps. *ACS Nano* **2022,** *16*, 13323-13338.
76. Skopintsev, P.; Ehrenberg, D.; Weinert, T.; James, D.; Kar, R. K.; Johnson, P. J. M.; Ozerov, D.; Furrer, A.; Martiel, I.; Dworkowski, F., et al., Femtosecond-to-Millisecond Structural Changes in a Light-Driven Sodium Pump. *Nature* **2020,** *583*, 314-318.
77. Mous, S.; Gotthard, G.; Ehrenberg, D.; Sen, S.; Weinert, T.; Johnson, P. J. M.; James, D.; Nass, K.; Furrer, A.; Kekilli, D., et al., Dynamics and Mechanism of a Light-Driven Chloride Pump. *Science* **2022,** *375*, 845-851.
78. Stockburger, M.; Klusmann, W.; Gattermann, H.; Massig, G.; Peters, R., Photochemical Cycle of Bacteriorhodopsin Studied by Resonance Raman Spectroscopy. *Biochemistry* **1979,** *18*, 4886-4900.
79. Saint Clair, E. C.; Ogren, J. I.; Mamaev, S.; Russano, D.; Kralj, J. M.; Rothschild, K. J., Near-IR Resonance Raman Spectroscopy of Archaerhodopsin 3: Effects of Transmembrane Potential. *J. Phys. Chem. B* **2012,** *116*, 14592-14601.
80. Shionoya, T.; Mizuno, M.; Tsukamoto, T.; Ikeda, K.; Seki, H.; Kojima, K.; Shibata, M.; Kawamura, I.; Sudo, Y.; Mizutani, Y., High Thermal Stability of Oligomeric Assemblies of Thermophilic Rhodopsin in a Lipid Environment. *J. Phys. Chem. B* **2018,** *122*, 6945-6953.

81. Kralj, J. M.; Spudich, E. N.; Spudich, J. L.; Rothschild, K. J., Raman Spectroscopy Reveals Direct Chromophore Interactions in the Leu/Gln105 Spectral Tuning Switch of Proteorhodopsins. *J. Phys. Chem. B* **2008,** *112*, 11770-11776.
82. Alshuth, T.; Stockburger, M.; Hegemann, P.; Oesterhelt, D., Structure of the Retinal Chromophore in Halorhodopsin. *FEBS Lett.* **1985,** *179*, 55-59.
83. Maeda, A.; Ogurusu, T.; Yoshizawa, T.; Kitagawa, T., Resonance Raman Study on Binding of Chloride to the Chromophore of Halorhodopsin. *Biochemistry* **1985,** *24*, 2517-2521.
84. Diller, R.; Stockburger, M.; Oesterhelt, D.; Tittor, J., Resonance Raman Study of Intermediates of the Halorhodopsin Photocycle. *FEBS Lett.* **1987,** *217*, 297-304.
85. Mizuno, M.; Nakajima, A.; Kandori, H.; Mizutani, Y., Structural Evolution of a Retinal Chromophore in the Photocycle of Halorhodopsin from *Natronobacterium pharaonis*. *J. Phys. Chem. A* **2018,** *122*, 2411–2423.
86. Gerscher, S.; Mylrajan, M.; Hildebrandt, P.; Baron, M.-H.; Müller, R.; Engelhard, M., Chromophore−Anion Interactions in Halorhodopsin from *Natronobacterium pharaonis* Probed by Time-Resolved Resonance Raman Spectroscopy. *Biochemistry* **1997,** *36*, 11012-11020.
87. Kajimoto, K.; Kikukawa, T.; Nakashima, H.; Yamaryo, H.; Saito, Y.; Fujisawa, T.; Demura, M.; Unno, M., Transient Resonance Raman Spectroscopy of a Light-Driven Sodium-Ion-Pump Rhodopsin from *Indibacter Alkaliphilus*. *J. Phys. Chem. B* **2017,** *121*, 4431-4437.
88. Nakamura, T.; Shinozaki, Y.; Otomo, A.; Urui, T.; Mizuno, M.; Abe-Yoshizumi, R.; Hashimoto, M.; Kojima, K.; Sudo, Y.; Kandori, H., et al., Unusual Vibrational Coupling of the Schiff Base in the Retinal Chromophore of Sodium Ion-Pumping Rhodopsins. *J. Phys. Chem. B* **2024,** *128*, 7813-7821.
89. Sasaki, J.; Brown, L.; Chon, Y.; Kandori, H.; Maeda, A.; Needleman, R.; Lanyi, J., Conversion of Bacteriorhodopsin into a Chloride Ion Pump. *Science* **1995,** *269*, 73-75.
90. Inoue, K.; Nomura, Y.; Kandori, H., Asymmetric Functional Conversion of Eubacterial Light-Driven Ion Pumps. *J. Biol. Chem.* **2016,** *291*, 9883-9893.
91. Hasemi, T.; Kikukawa, T.; Kamo, N.; Demura, M., Characterization of a Cyanobacterial Chloride-Pumping Rhodopsin and Its Conversion into a Proton Pump. *J. Biol. Chem.* **2016,** *291*, 355-362.
92. Marín, M. d. C.; Konno, M.; Yawo, H.; Inoue, K., Converting a Natural-Light-Driven Outward Proton Pump Rhodopsin into an Artificial Inward Proton Pump. *J. Am. Chem. Soc.* **2023,** *145*, 10938-10942.
93. Natarajan, C.; Signore, A. V.; Bautista, N. M.; Hoffmann, F. G.; Tame, J. R. H.; Fago, A.; Storz, J. F., Evolution and Molecular Basis of a Novel Allosteric Property of Crocodilian Hemoglobin. *Curr. Biol.* **2023,** *33*, 98-108.e4.
94. Sang, D.; Pinglay, S.; Wiewiora, R. P.; Selvan, M. E.; Lou, H. J.; Chodera, J. D.; Turk, B. E.; Gümüş, Z. H.; Holt, L. J., Ancestral Reconstruction Reveals Mechanisms of ERK Regulatory Evolution. *eLife* **2019,** *8*, e38805.
95. Chiang, C.-H.; Wymore, T.; Rodríguez Benítez, A.; Hussain, A.; Smith, J. L.; Brooks, C. L.; Narayan, A. R. H., Deciphering the Evolution of Flavin-Dependent Monooxygenase Stereoselectivity Using Ancestral Sequence Reconstruction. *Proc. Natl. Acad. Sci. USA* **2023,** *120*, e2218248120.
96. Sephus, C. D.; Fer, E.; Garcia, A. K.; Adam, Z. R.; Schwieterman, E. W.; Kacar, B., Earliest Photic Zone Niches Probed by Ancestral Microbial Rhodopsins. *Mol. Biol. Evol.* **2022,** *39*, msac100.